Improving the penetration depth in multiphoton excitation laser scanning microscopy

G. McConnell
University of Strathclyde
Strathclyde Institute for Pharmacy and Biomedical Sciences
Centre for Biophotonics
27 Taylor Street
Glasgow G4 0NR, United Kingdom

Abstract. More than a threefold increase in multiphoton laser scanning microscopy depth penetration using a passive predispersion compensation system is reported. Using dispersion-controlled pulses to counteract the effects of positive group delay dispersion in the imaging platform, optical sectioning of fluorescent samples to depths in excess of 800 μm was observed, compared with only 240 μm using a noncompensated setup. Experimental results obtained from both the predispersion compensated and noncompensated systems are compared with theoretical values of pulse broadening in a laser scanning microscope. The observed improvement in depth profiling potentially widens the applications and user base of nonlinear microscopy techniques.
[DOI: 10.1117/1.2360593]

Keywords: nonlinear; microscopy; laser; fiber; dispersion.

Paper 05382RR received Dec. 20, 2005; revised manuscript received May 24, 2006; accepted for publication May 25, 2006; published online Oct. 17, 2006.

1 Introduction

Multiphoton excitation laser scanning microscopy (MPLSM) has rapidly become a powerful method of performing high-resolution optical sectioning of fluorescing samples. Key to the success of this technique is the application of an ultrashort pulsed laser source that contributes the necessarily high peak intensity required for simultaneous absorption of two or more photons by the sample. The number of two-photon absorption events N is given by[1]

$$N\alpha\frac{\delta\cdot P_{av}^2}{\tau\cdot\Delta\upsilon^2}\cdot\left(\frac{NA^2}{2\cdot\hbar\cdot c\cdot\lambda}\right)^2 \tag{1}$$

where δ is the two-photon absorption cross-section, P_{av} is the average power of the laser, $\Delta\upsilon$ is the repetition rate of the laser source, τ is the pulse duration, and NA is the numerical aperture of the microscope objective lens. Only within the small focal volume is the peak intensity sufficiently high to provide nonlinear absorption, while the out-of-focus light intensity is inadequate to generate fluorescence from the sample. This enables simple, apertureless optical sectioning.[2] The repetition rate of the laser source is typically fixed at $\Delta\upsilon$=80 MHz. This is chosen to best match the fluorescence recovery lifetime of most fluorophores, thereby maximizing the efficiency of the process. The spot-size of the focused laser is prescribed in MPLSM by the NA of the objective lens applied and the wavelength of light. The objective lens and the wavelength of light are both chosen to match the application. Equation (1) suggests that the simplest method of increasing the peak intensity at the sample would be to increase the average power of the exciting source. In practice, however, increasing the average power can lead to undesirable thermal heating of the sample and, in the case of live cell and tissue imaging, can compromise the viability of the specimen.[3] For MPLSM, it is therefore important to restrict the average power applied to the sample. The effect of varying the remaining parameter, the pulse duration τ of the excitation source, has been shown to offer a solution.[4,5]

The difficulty in using ultrashort pulsed laser sources for MPLSM is undoubtedly minimizing the effects of positive dispersion to retain the necessarily short pulse duration at the focal plane within the sample.[6] From Fourier theory, a pulse of light comprises a range of wavelengths. Each of these wavelength components propagates with a different velocity. The dispersion D of the medium in which the light travels ultimately determines the magnitude of pulse broadening resulting from this variation in propagating velocity.[7] The broadened pulse is described by[8]

$$\tau_{\text{out}}=\tau_{\text{in}}\cdot\left[1+7.68\cdot\frac{(D\cdot L)^2}{\tau_{in}^4}\right]^{\frac{1}{2}} \tag{2}$$

where L is the optical path length, τ_{in} is the input pulse duration, and τ_{out} is the broadened output pulse duration. The factor of 7.68 is based on the assumption of Gaussian pulses.[8] In a laser scanning microscope system, the dispersion D arises from all optical components interacting with the excitation laser source, i.e., steering optics, scan mirrors, and the microscope objective lens. The value of D for a laser scanning microscope has been estimated as approximately $D\sim 3000-20{,}000$ fs^2/cm,[4,5,9] values that contribute toward significant pulse broadening. A sample of input pulse and output pulse durations associated with this range of D for a laser scanning microscope are calculated using Eq. (2) and presented in Fig. 1. Although it is clear that the pulse broadening

Address all correspondence to: Tel.: +44-141-548-4805; Fax: +44-141-548-4887; E-mail: g.mcconnell@strath.ac.uk

1083-3668/2006/11(5)/054020/7/$22.00 © 2006 SPIE

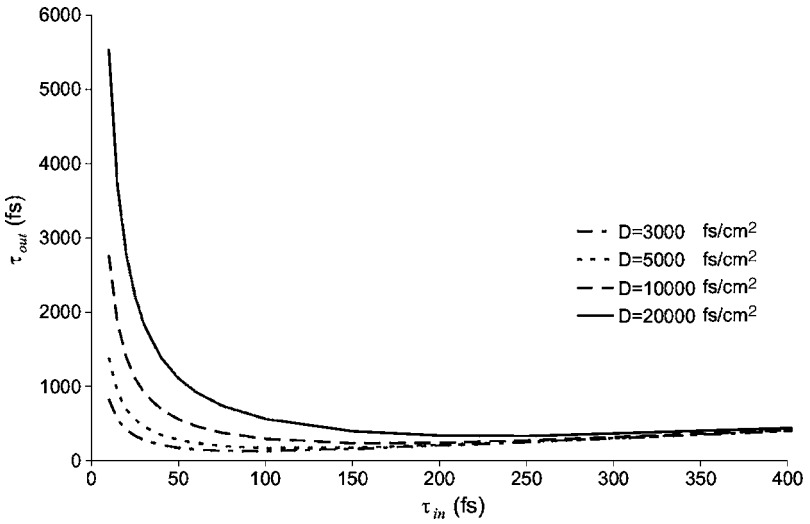

Fig. 1 Variation of output pulse durations with input pulse duration across a range of dispersion values for a laser scanning microscope. The percentage increase in output pulse duration as a result of dispersion is more pronounced for short input pulses, but the probability of instigating a two-photon absorption event decreases for longer pulses.

is most extreme for the shorter input pulses, there also exists a trade-off in using pulses that are too long and that do not have sufficient peak intensity to instigate multiphoton absorption.

Schemes that compensate for dispersion of laser scanning microscope systems can provide a solution to the detrimental effects of pulse broadening. Such systems typically involve adding a variable amount of negative dispersion into the path of the excitation beam (normally before the laser scanning system, thus constituting predispersion compensation) to counteract the positive dispersion experienced by the pulse. Several methods of predispersion compensation systems have been reported. These include the prism pair compressor used with a standard Ti:Sapphire laser, but the pulse duration of the system is limited to $\tau > 30$ fs and requires substantial modification to the laser geometry.[10] It is also possible to use a step-index silica-fiber-based compression scheme with an amplified Ti:Sapphire laser, but this is a rather expensive and photon-inefficient solution.[11] More recently, the application of a simple photonic crystal fiber-based predispersion compensation system was reported to successfully overcome these limitations.[12] By minimizing the pulse duration at the focal plane using this approach, an increase in fluorescence yield from thin samples of up to a factor of eight was reported.[13]

Although the dispersion of the imaging system is significant, the dispersion contributed by the sample in MPLSM is typically negligible in comparison. Where live cell or low concentration dye solutions are to be imaged, one can approximate the sample to that of water. The measurements of van Engen et al.[14] employed white-light interferometry to determine the dispersion of water to be approximately $D = 0.1$ fs^2/cm. From Eq. (2), even for input pulses as short as 10 fs, the increase in pulse duration on propagation through a 1-mm-thick sample of water is calculated to be substantially less than 1%. This correlates with the findings of Brakenhoff et al., where the pulse duration in the sample was demonstrated to be virtually unchanged on propagation through a range of specimens.[15]

As well as scatter and linear absorption within the sample,[16] one of the limiting factors on the depth of imaging possible with MPLSM is the reduction in peak intensity due to the increase in pulse duration arising from dispersion within the laser scanning microscope. With the application of a predispersion compensation system that realizes very short pulse durations at the focal plane, one can provide a higher peak intensity at the sample surface.[13] On propagating through the sample, one can assume that since the pulse duration is largely unchanged, the high propagating peak intensity of the excitation source should be retained deeper within the sample. Hypothetically, this should increase the resolvable depth of MPLSM, enabling deeper optical sectioning.

In this paper, this hypothesis is tested and, using a passive and modular predispersion compensation system, more than a threefold increase in MPLSM depth penetration when compared with a noncompensated system is experimentally demonstrated. Using dispersion-controlled pulses to counteract the effects of positive dispersion in the imaging system enabled depth penetration of >800 μm in a fluorescent dye solution, compared with only 240 μm using a noncompensated setup. Similarly, fluorescent tissue samples imaged using the predispersion compensation system offered a threefold improvement in depth resolution. This enhancement in depth profiling uses entirely commercially available components in a simple and robust modular accompaniment to existing MPLSM instrumentation and, furthermore, does not require active control. This novel approach to extending the depth resolution of MPLSM potentially widens the applications and user base of nonlinear microscopy techniques. Experimental results obtained from both the predispersion compensated and noncompensated systems are presented along with simple theoretical models of pulse propagation through a turbid sample.

2 Experiment

The experimental setup is shown schematically in Fig. 2. A Ti:Sapphire laser (Mira 900-F, Coherent) typically applied for

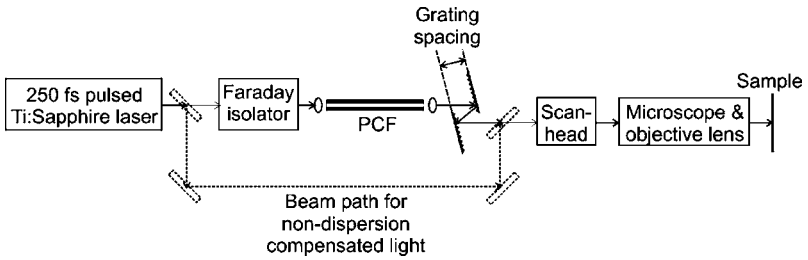

Fig. 2 Simple schematic diagram of the predispersion-compensated system. A 250-fs pulsed source was propagated through a 30-dB Faraday isolator and the resultant radiation focused into a section of photonic crystal fiber (PCF). The output radiation was collimated and propagated through a grating pair with variable spacing between the elements. The resultant source was then either characterized using diagnostic instrumentation or toward the laser scanning microscope to perform MPLSM. This could easily be compared with the nondispersion-compensated system using an alternative beam path.

MPLSM was used as the platform source. This system delivered pulses of approximately $\tau \sim 250$-fs duration across a tunable wavelength range of $\lambda = 710-890$.[12] For the purposes of this investigation, the wavelength was tuned to $\lambda = 830$ nm, with a spectral full-width at half-maximum of $\Delta\lambda = 7$ nm. The pulse repetition rate was $\Delta\upsilon = 76$ MHz, and at the emission wavelength peak, the average power was measured to be $P_{av} \sim 450$ mW. When ordinarily applied for MPLSM, the average power of the source is heavily attenuated to minimize sample heating. For these experiments, the Ti:Sapphire laser beam was propagated through a 30-dB Faraday isolator to reduce the effect of feedback from further optical components in the setup. This beam was then focused using a miniature aspheric lens of focal length $f = 3.1$ mm and propagated into a 8.6-cm-length of photonic crystal fiber (PCF). The PCF is used to perform self-phase modulation of the input beam, resulting in a broadened spectral profile with a linear phase gradient across the pulse. The PCF (Crystal Fibre A/S) consisted only of silica and comprised a hexagonal structure of air holes to promote guiding in a 2.6-μm core. The distance between adjacent air holes was 1.8 ± 0.2 μm, and the hole diameter:separation ratio was approximately 0.35. This arrangement provided a high nonlinearity and a zero dispersion wavelength of approximately $\lambda_0 = 900$ nm. Across the operational range of the input Ti:Sapphire laser source, the PCF therefore possessed a low and positive dispersion and was consequently well-suited to performing pulse compression. From previous experiments,[12] the dispersion in the fiber used was estimated to be $D \sim 50$ ps/nm·km at 800 nm.

Using high-efficiency gratings, the resultant output was then used to compensate for dispersion not only present within the laser setup, but also crucially from the laser scanning microscope system and the sample. The output from the PCF was collimated using another $f = 3.1$-mm focal length aspheric lens element and was passed through a dispersion compensating stage, consisting of two parallel 600-lines/mm gratings separated by up to 16 mm. This grating pair provided a negative dispersion in the beam of $b_0 \cdot 0.463$ ps^2/m, where b_0 was the grating separation.[17] The efficiency of the grating pair at $\lambda = 830$ nm was measured to be $\sim 50\%$. The light transmitted by the grating pair was then passed into computer-controlled laser scanning system (MRC1024ES, Bio-Rad) that was coupled to an inverted microscope (TE300, Nikon). For comparison with the performance of the conventional Ti:Sapphire excitation source, the platform system could similarly be propagated into the laser scanning microscope system. In either case, the light entering the scan head was reflected and manipulated by a pair of highly reflecting scanning galvo mirrors toward the microscope. A 40× objective lens with a 1.3 numerical aperture oil-immersion microscope objective lens (Super Fluor, Nikon) was used to focus the radiation onto the fluorescently stained sample. Fluorescence resulting from two-photon excitation, using either the pre- or nondispersion-compensated Ti:Sapphire source, was collected by the same objective lens and propagated through an optical band-pass filter to reject reflected light from the exciting source. This fluorescence was then relayed to a sensitive photomultiplier tube housed within the scan head. This signal was used, along with image capture software, to visualize fluorescently stained regions of the chosen sample.

The primary sample investigated comprised of 2 μM fluorescein in water. From the measurements of van Engen et al. described previously,[14] the dispersion contributed by the sample is negligible. Consequently, for this investigation the dispersion of the laser scanning microscope has been conservatively estimated to be $D \sim 5000$ fs^2/cm[9], while the dispersion contributed by the sample has been neglected. Further images and measurements were made using a sample comprising guinea pig detrusor prepared with the fluorescent indicator Alexa 488 to ascertain the suitability of the predispersion compensation system for tissue imaging.

3 Results

The pulse duration and corresponding spectrum resulting from the optimized predispersion compensation system are shown in Figs. 3(a) and 3(b), respectively, with 200 mW of average power transmitted by the PCF. This corresponds to an efficiency of 44%. The pulse duration was measured using a collinear scanning autocorrelator with a GaAsP two-photon detector, which only had a two-photon response at $\lambda = 830$ nm. Low-dispersion mirrors were used in the autocorrelator and to steer the beam. The pulse duration shown in Fig. 3(a) corresponds to a grating spacing of 3 mm, where the shortest pulse duration was measured. This pulse duration was measured before entering the scan head and, therefore, this grating spacing does not correspond to that required to compensate for the dispersion within the laser scanning microscope. The spectral output from the PCF was captured and measured using an optical spectrum analyzer with a spectral

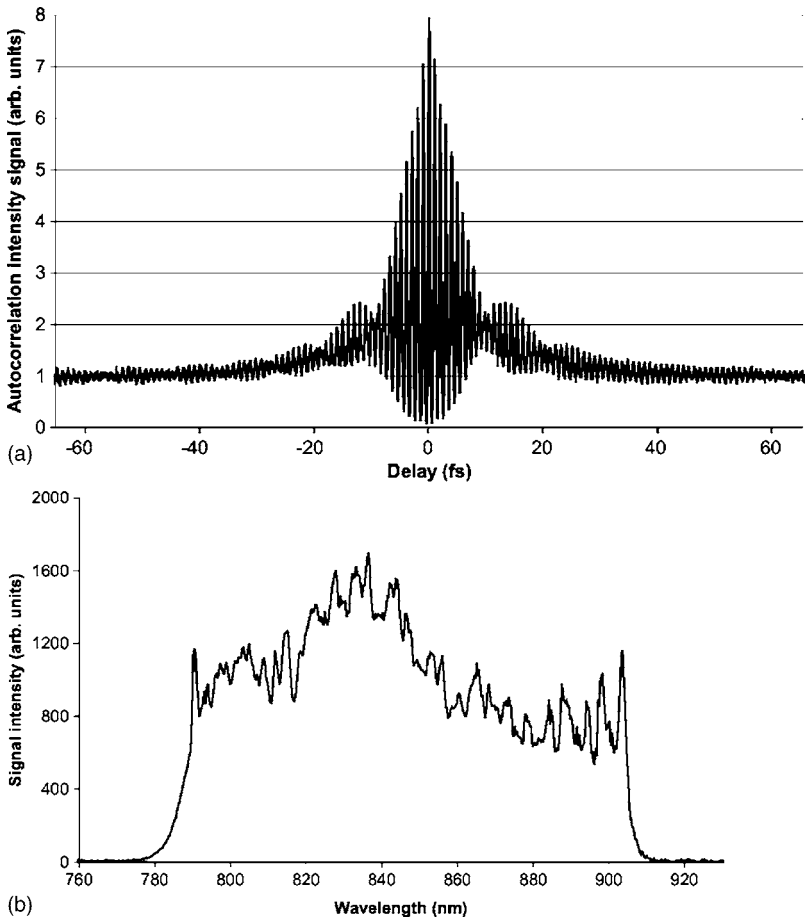

Fig. 3 (a) Two-photon autocorrelation of the output pulse measured after the grating pair and before the scan head. This minimum pulse duration of $\tau \sim 25$ fs corresponds to an optimum grating spacing of 3 mm. (b) Optical output spectrum resulting from the predispersion-compensation system, measured immediately after the PCF for an output power of $P_{av} \sim 200$ mW.

resolution of $\Delta\lambda = 1$ nm (USB2000, Ocean Optics). As expected, the spectrum [shown in Fig. 3(b)] did not vary with changing the grating spacing. Conveniently, the broadened spectrum covered the normal tuning range of a Ti:Sapphire laser, and therefore no specialist optical components were required to handle the predispersion compensated laser.

A comparison between the predispersion-compensated system and the noncompensated system was performed. First, the predispersion-compensated system was propagated into the scan head. The grating spacing was varied to provide the maximum fluorescence signal (and hence the shortest pulse duration) from a thin test sample comprising fluorescent beads of 100-μm diameter. The fluorescence signal was separated from the longer wavelength excitation radiation using a high-quality $\lambda = 540 \pm 30$ nm optical interference band-pass filter. The images were obtained using capture software (Lasersharp 2000 v5.2, Bio-Rad). Each image comprised 512*512 pixels and was obtained at a 0.95-Hz frame rate. The optimum grating spacing was determined to be 15 mm, which corresponded to a minimum pulse duration at the sample (estimated to be approximately $\tau \sim 40$ fs). Given that the average power at the sample was measured to be $P_{av} \sim 22$ mW, a peak power of approximately $P_{peak} \sim 6.8$ kW and a peak intensity of $I_{peak} \sim 100\ \mathrm{GW/cm^2}$ is calculated at the focal plane. Next, fluorescence contrast images of this thin sample were then captured and compared with the nondispersion-compensated system. The conventional Ti:Sapphire laser source was attenuated before being propagated into the scan head and checked to ensure that the same average power was delivered to the specimen. The comparative contrast images from the pre- and noncompensated sources are shown in Fig. 4(a) and 4(b), respectively. Clearly, the fluorescence signal from the predispersion-compensated system is higher than that from the nondispersion-compensated source. In fact, analysis using image processing software (Metamorph v4.6r3) revealed a factor of 6 increase in fluorescence signal intensity from this thin sample. This correlates with the postulated decrease in pulse duration at the focal plane.

To determine the effect of predispersion compensation on the resolvable depth, both the pre- and nondispersion-compensated systems were used in turn to obtain a 1-mm-thick stack of optical cross-sectional fluorescence contrast images from the aforementioned 2-μM fluorescein solution. Again, the fluorescence signal was separated from the longer wavelength excitation radiation, this time using a high-quality $\lambda = 525 \pm 25$-nm optical interference band-pass filter. Each image comprised 512^2 pixels and was obtained at a 0.95-Hz

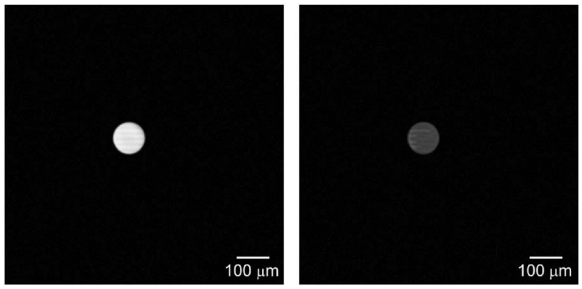

Fig. 4 Comparative contrast images of 100-μm-diameter fluorescent latex beads using the (a) pre- and (b) noncompensated sources. The fluorescence signal from the predispersion-compensated system was a factor of 6 greater than that from the nondispersion-compensated source.

frame rate and was averaged using a Kalman filter over four consecutive scans.

Images at depths of up to 820 μm for both the pre- and noncompensated systems, respectively, were obtained. The depth penetration of the predispersion-compensated system noticeably exceeds that of the noncompensated approach. The mean fluorescence intensity, calculated over $n=10$ samples for images taken at depths of up to 820 μm and for both methods are shown on a plot in Fig. 5. The maximum depth penetration for which a fluorescence intensity signal is obtained using the precompensated system reaches approximately 800 μm, compared with 240 μm for the nondispersion-compensated scheme. This threefold increase in resolvable depth is attributed to the application of the increased peak intensity radiation, arising from the predispersion-compensated pulses. Given the comparatively low dispersion contributed on propagation through the sample, there is no need for active control of the pulse duration within the sample. Instead, compensating for the dispersion arising from the laser scanning system, the microscope and the chosen objective lens provide the enhanced depth penetration and resolvable fluorescence.

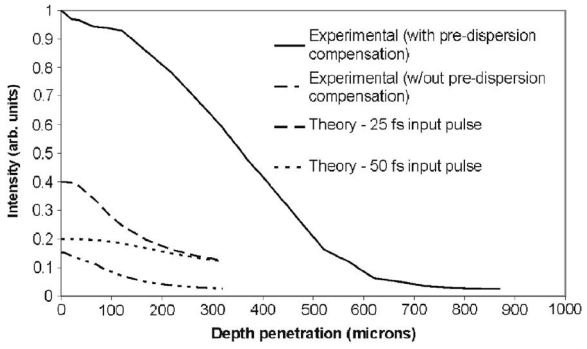

Fig. 5 Experimental and calculated fluorescence intensity based on various input pulse durations. The theoretical values are taken from the values calculated using Eqs. (1) and (2) and the results displayed in Fig. 1. The experimental values are based on results from optical cross-sectional fluorescence contrast images from a 2-μM concentration fluorescein solution obtained using both pre- and nondispersion-compensated excitation ($n=10$ samples at each depth). The depth penetration of the predispersion-compensated system approached 820 μm, while the nondispersion-compensated system provided fluorescence data to depths of only 240 μm. The significant increase in resolvable depth measured in these experiments is attributed to the application of the increased peak intensity radiation, arising from the predispersion-compensated pulses. This agrees well with the theoretical values, as shown.

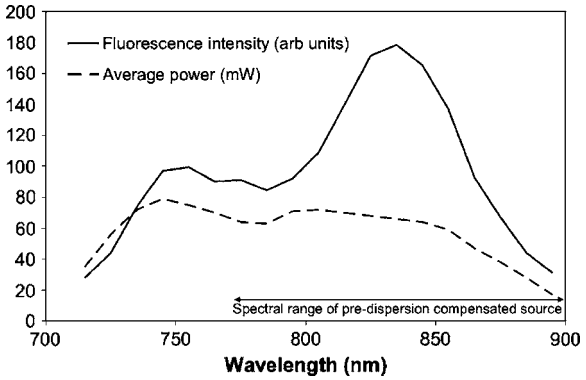

Fig. 6 Two-photon excitation spectrum of fluorescein using the nondispersion-compensated system. The fluorescence intensity maximum was observed close to the central maximum of the spectrally broadened excitation source at $\lambda=824$ nm. This infers that the predispersion-compensated source did therefore not provide new wavelengths that could better excite the specimen and that the increase in fluorescence is solely due to the decrease in pulse duration within the sample.

To make certain that this threefold enhancement in resolvable depth was not a consequence of the spectrally broadened output of the dispersion-compensated system's providing a better match for the excitation profile of the sample, the sample was excited using the nondispersion-compensated system across a wide wavelength range and the resultant fluorescence contrast image captured. The excitation power was kept constant across this spectral range by appropriately attenuating the source. The resultant mean fluorescence intensity across this wavelength range is shown in Fig. 6. The fluorescence-intensity maximum was observed at an excitation wavelength of $\lambda=824$ nm, which closely matches the central maximum of the spectrally broadened excitation source. This infers that the predispersion-compensated source therefore did not provide new wavelengths that could better excite the specimen and that the increase in fluorescence is solely due to the decrease in pulse duration within the sample.

As well as imaging a fluorescent dye solution, the systems were compared when imaging a more turbid fluorescently labeled tissue sample. A section of guinea pig detrusor was prepared with Alexa 488, a fluorescent nerve indicator, and DAPI, a DNA-specific label. Excitation of the fluorescently labeled nerves was executed using both the pre- and nondispersion-compensated laser sources at depths of up to 90 μm, in order to compare system performance. In each case, the fluorescence signal was discriminated from residual backscattered excitation radiation using a high-quality $\lambda=540\pm30$-nm optical interference band-pass filter. Again, a $40\times/1.3$ N.A. microscope objective lens was used. Each image comprised 512^2 pixels and was captured at a frame rate of 0.95 Hz and applying a Kalman averaging filter over four consecutive scans. In both instances, the average power reaching the sample was measured to be 27 mW.

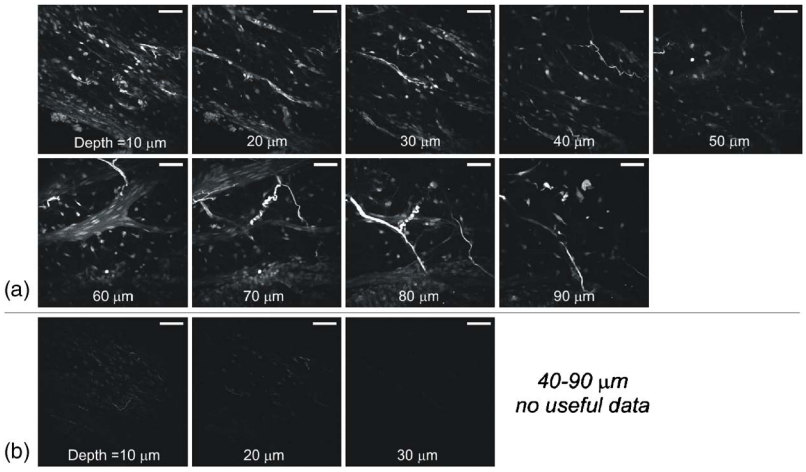

Fig. 7 Fluorescence contrast images from a section of guinea pig detrusor labeled with Alexa 488 and DAPI obtained using (a) pre- and (b) nondispersion-compensated excitation, both at an average power of 27 mW. The depth at which the image was taken is displayed on each image. Contrast images obtained at depths of up to 90 μm were captured using the predispersion-compensated system; however, the depth penetration of the noncompensated system at the same average power reached only 30 μm. The scale bar corresponds to 25 μm.

Typical images obtained at depths of up to 90 μm are shown in Figs. 7(a) and 7(b) for both the pre- and noncompensated systems, respectively. The fluorescence signal for the nondispersion-compensated system wanes at a depth of approximately 30 μm, whereas using the predispersion-compensated system, fluorescently labeled structures can still be resolved at depths of 90 μm. Over an imaging period in excess of an hour, no photo damage was observed. The passive predispersion-compensated system therefore extends the depth over which fluorescent media can be visualized using minimally-invasive MPLSM at moderate incident average powers.

4 Discussion

As well as demonstrating significant benefits for MPLSM, the results reported may also impact upon alternative nonlinear microscopy methods and nonlinear optical processes that use ultrashort pulsed laser sources. In the case of second harmonic generation imaging, for example, the use of shorter pulse durations at the focal plane would increase the generated signal. However, the spectral acceptance bandwidth of the sample under investigation may limit the efficiency of the process.[18] Similarly, the use of a spectrally broadened source may pose problems within spectral imaging, e.g., coherent anti-Stokes–Raman spectroscopic imaging, where the spectral bandwidth of the source determines the spectral resolution of the resultant contrast image.[19] Therefore, although a very short pulse duration at the focal plane can greatly increase the depth over which optical sectioning may occur, one must also consider the effects of the spectral bandwidth of the source.

As with all MPLSM, care should be taken to minimize the dose of light to the specimen. This is of particular concern for live cell imaging, but peak intensity sources of around $I_{peak} \sim 200\ \mathrm{GW/cm^2}$ have shown to preserve sample viability over long imaging periods.[20] Perhaps less of a concern is the growing use of MPLSM methods for the characterization of other structures, including semiconductor samples.[21] Typically, these materials have significantly higher damage thresholds. Furthermore, this predispersion-compensation system may provide a useful route to perform spatially localized optically beam-induced current for nondestructive semiconductor testing, providing information from deeper within the sample than is presently possible.

The scan head used in this study was a very basic type and did not comprise additional optics that would contribute toward higher dispersion, for example, low-quality optical filters, highly dispersive mirrors, or electro-optic or acousto-optic modulators (EOM and AOM). Such EOM or AOM systems are commonly applied to MPLSM to control the average power of the laser source applied to the sample at increasing depths. However, the inclusion of such an AOM may contribute dispersion in excess of $D \sim 12{,}000\ \mathrm{fs^2/cm}$.[22] Given the standard $\tau \sim 150$-fs pulsed commercial Ti:Sapphire lasers commonly applied to MPLSM, the addition of an AOM corresponds to an increase in pulse duration of up to $\tau \sim 270$ fs. Based on the results presented, this increase would further impede the depth resolution. Hence, the application of this passive predispersion compensation would present an advantage with alternative laser scanning microscope systems.

5 Conclusion

In conclusion, the application of a simple passive predispersion compensation has enabled greater than a three-time increase in the depth over which MPLSM can be performed. Using dispersion-controlled pulses to counteract the effects of group delay dispersion in the laser scanning microscope system enabled depth penetration of over 800 μm in standard dye samples, compared with only 240 μm using a nondispersion-compensated setup. A good overlap between these experimental values and those calculated from theory is indicative that this approach will enable imaging of a wide range of samples at greater depths. Indeed, the depth over which a fluorescently labeled tissue sample was imaged-increased threefold on the application of predispersion compensation. This novel and simple approach to enhancing the depth-profiling capability of MPLSM potentially widens the

applications and user base of nonlinear microscopy techniques. Furthermore, since this enhancement in depth profiling does not rely upon actively controlled elements, the predispersion-compensation system also offers the potential for increased depth profiling via video-rate MPLSM.

Acknowledgments

The author acknowledges support from the Royal Society of Edinburgh.

References

1. A. Diaspro and M. Robello, "Two-photon excitation of fluorescence for three-dimensional optical imaging of biological structures," *J. Photochem. Photobiol., A* **55**, 1–8 (2000).
2. W. Denk, J. H. Strickler, and W. W. Webb, "Two-photon laser scanning fluorescence microscope," *Science* **248**, 73–76 (1990).
3. A. Schönle and S. W. Hell, "Heating by absorption in the focus of an objective lens," *Opt. Lett.* **23**, 325–327 (1998).
4. M. Müller, J. Squier, R. Wolleschensky, U. Simon, and G. J. Brakenhoff, "Dispersion precompensation of 15 femtosecond optical pulses for high-numerical-aperture objectives," *J. Microsc.* **191**, 141–150 (1998).
5. J. Squier, V. V. Yakovlev, M. Müller, A. Buist, G. J. Brakenhoff, and U. Simon, "Measurement and modeling of the focusing of 15 femtosecond optical pulses with a high-numerical-aperture objective," *Proc. Society Photo-Optical Instrumentation Engineers (SPIE)*, 18–21 (1998).
6. Z. Bor, "Distortion of femtosecond pulses in lenses and lens systems," *J. Mod. Opt.* **35**, 1907–1918 (1988).
7. E. Hecht and A. Zajac, *Optics*, Addison-Wesley, New York (2003).
8. J. C. Diels and W. Rudolph, *Ultrashort Laser Pulse Phenomena: Fundamentals, Techniques and Applications on a Femtosecond Time Scale*, Academic Press, San Diego (1996).
9. K. Koenig, "Multiphoton microscopy in life sciences," *J. Microsc.* **200**, 83–104 (2000).
10. S. Lakó, J. Seres, P. Apai, J. Balzás, R. S. Windeler, and R. Szipőcs, "Pulse compression of nanojoule pulses in the visible using microstructure optical fiber and dispersion compensation," *Appl. Phys. B* **76**, 267–275 (2003).
11. A. Shirakawa, I. Sakane, and T. Kobayashi, *Ultrafast Phenomena XI*, Springer, Heidelberg (1998).
12. G. McConnell and E. Riis, "Ultra-short pulse compression using photonic crystal fibre," *Appl. Phys. B* **78**, 557–563 (2004).
13. G. McConnell and E. Riis, "Two-photon laser scanning microscopy using photonic crystal fibre," *J. Biomed. Opt.* **9**, 922–927 (2004).
14. A. G. van Engen, S. A. Diddams, and T. S. Clement, "Dispersion measurements of water with white-light interferometry," *Appl. Opt.* **37**, 5679–5686 (1998).
15. G. J. Brakenhoff, M. Müller, and J. Squier, "Femtosecond pulse-width control in microscopy by 2-photon absorption autocorrelation," *J. Microsc.* **179**, 253–260 (1995).
16. J. B. Pawley, "Laser sources for confocal microscopy," in *Handbook of Biological Confocal Microscopy*, pp. 69–97, Plenum, New York (1995).
17. W. J. Tomlinson, R. H. Stolen, and C. V. Shank, "Compression of optical pulses chirped by self-phase modulation in fibers," *J. Opt. Soc. Am. B* **1**, 139–149 (1984).
18. G. P. Agrawal and R. Boyd, *Contemporary Nonlinear Optics (Quantum Electronics: Principles and Applications)*, Academic Press, London (1992).
19. A. Volkmer, "Vibrational imaging and microspectroscopies based on coherent anti-Stokes Raman scattering microscopy," *J. Appl. Phys.* **38**, 59–81 (2005).
20. J. M. Squirrell, D. L. Wokosin, J. G. White, and B. D. Bavister, "Long-term two-photon fluorescence imaging of mammalian embryos without compromising viability," *Nat. Biotechnol.* **17**, 763–767 (1999).
21. S. A. Blanton, M. A. Hines, M. E. Schmidt, and P. Guyot-Sionnest, "Two-photon spectroscopy and microscopy of II-VI semiconductor nanocrystals," *J. Lumin.* **70**, 253–268 (1996).
22. V. Iyer, B. E. Losavio, and P. Saggau, "Compensation of spatial and temporal dispersion for acousto-optic multiphoton laser-scanning microscopy," *J. Biomed. Opt.* **8**, 460–471 (2003).